British Journal of Pharmacology (2001) 134, 305–312

www.nature.com/bjp

Neuronal nitric oxide synthase (NOS) regulates leukocyte-endothelial cell interactions in endothelial NOS deficient mice

*,[1]Maria-Jesus Sanz, [1]Michael J. Hickey, [1]Brent Johnston, [1]Donna-Marie McCafferty, [1]Eko Raharjo, [2]Paul L. Huang & [1]Paul Kubes

[1]Immunology Research Group, University of Calgary, Calgary, Alberta T2N 4N1, Canada and [2]Harvard Medical School, Cardiovascular Research Center, Massachusetts General Hospital, Charlestown, Massachusetts, MA 02129, U.S.A.

1 The present study was designed to examine the possible role of neuronal nitric oxide synthase (nNOS) in regulation of leukocyte–endothelial cell interactions in the absence of endothelial nitric oxide synthase (eNOS), using intravital microscopy of the cremasteric microcirculation of eNOS$^{-/-}$ mice.

2 Baseline leukocyte rolling and adhesion revealed no differences between wild-type and eNOS$^{-/-}$ mice in either the cremasteric or intestinal microcirculations.

3 Superfusion with L-NAME (100 μM) caused a progressive and significant increase in leukocyte adhesion in both wild-type and eNOS$^{-/-}$ mice, without detecting differences between the two strains of mice.

4 Superfusion with 7-nitroindazole (100 μM), a selective inhibitor of nNOS, had no effect on leukocyte adhesion in wild-type animals. However, it increased leukocyte adhesion significantly in eNOS$^{-/-}$ mice, which was reversed by systemic L-arginine pre-administration.

5 Stimulation of the microvasculature with H_2O_2 (100 μM) induced a transient elevation in leukocyte rolling in wild-type mice. Conversely, the effect persisted during the entire 60 min of experimental protocol in eNOS$^{-/-}$ mice either with or without 7-nitroindazole.

6 Semi-quantitative analysis by RT–PCR of the mRNA for nNOS levels in eNOS$^{-/-}$ and wild-type animals, showed increased expression of nNOS in both brain and skeletal muscle of eNOS$^{-/-}$ mice.

7 In conclusion, we have demonstrated that leukocyte-endothelial cell interactions are predominantly modulated by eNOS isoform in postcapillary venules of normal mice, whereas nNOS appears to assume the same role in eNOS$^{-/-}$ mice. Interestingly, unlike eNOS there was insufficient NO produced by nNOS to overcome leukocyte recruitment elicited by oxidative stress, suggesting that nNOS cannot completely compensate for eNOS.

British Journal of Pharmacology (2001) **134,** 305–312

Keywords: NO; eNOS; nNOS; leukocyte; endothelium; hydrogen peroxide; eNOS$^{-/-}$ mice; intravital microscopy

Abbreviations: Dv, venular diameter; eNOS, endothelial nitric oxide synthase; H_2O_2, hydrogen peroxide; L-NAME, N^G-nitro-L-arginine methyl ester; nNOS, neuronal nitric oxide synthase; NO, nitric oxide; NOS, NO synthase; V_{mean}, mean red blood cell velocity; V_{rbc}, centreline red blood cell velocity; V_{wbc}, leukocyte rolling velocity

Introduction

Nitric oxide (NO) can be synthesized by three different isoforms of NO synthase (NOS), namely, neuronal NOS (nNOS or NOS1), inducible NOS (iNOS or NOS2) and endothelial NOS (eNOS or NOS3). nNOS and eNOS are constitutively expressed and respond to calcium-calmodulin signalling. Constitutive production and release of NO plays a major role in vascular homeostasis, being central to the regulation of blood pressure, blood flow, platelet aggregation and leukocyte adhesion (Moncada *et al*., 1991, Radomski *et al*., 1987, Kubes *et al*., 1991). In 1991, it was demonstrated that inhibition of NO production with a non-specific inhibitor of NOS induced an increase in leukocyte adhesion in postcapillary venules that was unrelated to reduction in shear rates but dependent upon the adhesion molecule CD11/CD18 (Kubes *et al*., 1991). Davenpeck *et al*. (1994) showed that inhibition of endogenous NO production results in the upregulation of the adhesion molecule P-selectin on the endothelial surface of mesenteric venules. In addition, subsequent work both *in vitro* and *in vivo* revealed that the increased adhesion associated with reduced nitric oxide production was related to an increase in oxidative stress (Niu *et al*., 1996, Kubes *et al*., 1993). Indeed, delivery of exogenous NO could reduce superoxide as well as H_2O_2-dependent leukocyte adhesion (Gaboury *et al*., 1993, Johnston *et al*., 1996). Although it was always assumed that the isoform of NOS responsible for these effects was endothelial in origin, this has never been confirmed.

Recent studies with eNOS-deficient (eNOS$^{-/-}$) mice have revealed that there is an increase in systemic blood pressure and some increase in baseline leukocyte rolling and adhesion, particularly in response to acute inflammatory mediators, as well as increased neutrophil recruitment at sites of myocardial

*Author for correspondence: Departamento de Farmacología, Facultad de Medicina, Universidad de Valencia, Av. Blasco Ibañez, 15–17 46010 Valencia, Spain; E-mail: maria.j.sanz@uv.es

ischemia/reperfusion injury (Huang *et al*., 1995, Lefer *et al*., 1999, Jones *et al*., 1999). These observations suggest that functions mediated by NO produced by eNOS are not replaced by an alternative NOS isoform in these mice. In contrast, evidence from several studies suggests that in mice which are genetically deficient in one of the constitutive NOS isoforms, the remaining constitutive isoform assumes some of the functions normally attributable to the deleted enzyme. For example, inhibition of eNOS in nNOS-deficient ($nNOS^{-/-}$) mice results in a larger infarction size after cerebral ischemia, suggesting some interplay between the two isoforms (Huang *et al*., 1994). Moreover, arterioles from the pial circulation of $eNOS^{-/-}$ mice respond normally to endothelial-dependent vasodilators *via* NO produced by nNOS (Meng *et al*., 1996). Similarly, penile erection, which is thought to be dependent on nNOS-derived NO, is not compromised in $nNOS^{-/-}$ mice, but is mediated by eNOS-derived NO (Burnett *et al*., 1996). These observations suggest that for vasodilation, NO from both nNOS and eNOS provide mutually compensating pathways. Therefore, it is conceivable that modulation of leukocyte-endothelial cell interactions by NO could be subjected to the same compensating mechanisms in mice lacking eNOS.

Thus, the aim of the present study was to examine the relative importance of eNOS and nNOS in the regulation of leukocyte-endothelial cell interactions *in vivo*, specifically in $eNOS^{-/-}$ mice. To achieve this aim we used intravital microscopy to visualize these interactions in the microvasculatures of the cremaster muscle and the small intestinal submucosa of wild-type and $eNOS^{-/-}$ mice. In initial experiments we compared baseline leukocyte trafficking in the two strains of mice. To further define the relative roles of each NOS isoform in regulation of these interactions we performed additional experiments with L-NAME, a non-selective NOS inhibitor, and 7-nitroindazole, a selective inhibitor of nNOS. In a final series of experiments we compared the alterations in leukocyte rolling in wild-type and $eNOS^{-/-}$ mice induced by exposure to the oxidant hydrogen peroxide. The findings indicate that in wild-type mice, eNOS has a dominant role in ongoing modulation of leukocyte-endothelial cell interactions, whereas in $eNOS^{-/-}$ mice, nNOS assumes this function.

Methods

Animals

Male eNOS-deficient mice were generated on a background of mixed C57BL/6 × 129/Sv as described previously (Huang *et al*., 1995). Wild-type mice of the same background (C57BL/6/129Sv) were used as controls. All animals were employed between 6–10 weeks of age.

Intravital microscopy

The mouse cremaster preparation used in this study was similar to that described previously (Hickey *et al*., 1999). Mice were anaesthetized by i.p. injection with a mixture of xylazine hydrochloride (10 mg kg^{-1}) and ketamine hydrochloride (200 mg kg^{-1}). A polyethylene catheter was placed in the jugular vein to permit the intravenous administration of additional anaesthetic. The cremaster muscle was dissected free of tissues and exteriorized onto an optical clear viewing pedestal. The muscle was cut longitudinally with a cautery and held flat against the pedestal by attaching silk sutures to the corners of the tissue. The muscle was then perfused continuously at a rate of 1 ml min^{-1} with warmed bicarbonate-buffered saline (pH 7.4).

The cremasteric microcirculation was then observed by using an intravital microscope (Optiphot-2; Nikon, Mississauga, Canada) equipped with a 25 × objective lens (Wetzlar L25/0.35; E. Leitz, Munich, Germany) and a 10 × eyepiece. A video camera (Panasonic 5100 HS, Osaka, Japan) mounted on the microscope projected the image onto a colour monitor and the images were video recorded for playback analysis. Single unbranched cremasteric venules (20–40 μm in diameter) were selected for study and the diameter was measured on-line by using a video caliper (Microcirculation Research Institute, Texas A&M University, College Station, Texas). Centreline red blood cell velocity (V_{rbc}) was also measured on-line by using an optical Doppler velocimeter (Microcirculation Research Institute). Venular blood flow was calculated from the product of mean red blood cell velocity ($V_{mean} = V_{rbc}\ 1.6^{-1}$) and cross sectional area, assuming cylindrical geometry. Venular wall shear rate (γ) was calculated based on the Newtonian definition: $\gamma = 8 \times (V_{mean}\ D_v^{-1})\ s^{-1}$, in which D_v is venular diameter (House & Lipowsky, 1987).

The number of rolling, adherent and emigrated leukocytes was determined off-line during playback of videotaped images. Rolling leukocytes were defined as those white blood cells moving at a velocity less than that of erythrocytes in the same vessel. Leukocyte rolling velocity (V_{wbc}) was determined from the time required for a leukocyte to move along 100 μm length of the microvessel and is expressed as $\mu m\ s^{-1}$. Flux of rolling leukocytes was measured as those cells that could be seen moving past a defined reference point in the vessel. The same reference point was used throughout the experiment because leukocytes may roll for only a section of the vessel before rejoining the blood flow or becoming firmly adherent. A leukocyte was defined as adherent to venular endothelium if it was stationary for at least 30 s. Leukocyte adhesion was expressed as the number per 100 μm length of venule.

The mouse small intestinal preparation was carried out as previously performed (Massberg *et al*., 1998). Briefly, following anaesthesia and cannulation of the jugular vein as already described, the animals were placed in a supine position on a heating pad (TR-100 temperature controller, Fine Science Tools Inc., Vancouver, Canada) for maintenance of body temperature at 37°C. The abdomen was then opened transversely and a segment of the jejunum, close to the ileo-cecal valve, was gently exteriorized and placed on a specially designed adjustable stage. The exposed segment was then covered with a glass coverslip and constantly superfused with warmed bicarbonate-buffered saline (pH 7.4).

The submucosal microcirculation was visualized after intravenous injection of 0.05 ml 5% fluorescein isothiocyanate (FITC)-labelled dextran. Leukocytes were stained *in vivo* by intravenous injection of 0.1 ml 0.05% rhodamine-6G per animal. Then the exposed segment of the intestine was analysed by epi-illumination technique using an intravital microscope (Optiphot-2; Nikon, Mississauga, Canada) with a 20 × water immersion objective lens (Nikon SLDW, Tokyo,

Japan) and a 10× eyepiece. A CCD video camera (Pieper GMBH, FK 6990, Schwarte, Germany) mounted on the microscope projected the image onto a colour monitor, and images were recorded for playback analysis using a videocassette recorder. Rhodamine-6G-associated fluorescence was visualized by epi-illumination at 510–560 nm, using a 590 nm emission filter. FITC-dextran-associated fluorescence was also detected by epi-illumination with an excitation wavelength: 450–490 nm and emission wavelength of 520 nm. The diameter of the vessel was measured on-line by using a video caliper (Microcirculation Research Institute). The number of rolling and adherent leukocytes were determined off-line during playback of videotaped images and expressed as previously described for the cremasteric preparation.

Experimental protocol

To determine basal differences in haemodynamic and leukocyte parameters between wild-type and eNOS$^{-/-}$ mice, both the cremaster muscle and the small intestine submucosa were examined. Separate groups of mice were examined for each tissue. In each experiment, data were collected at 0, 30 and 60 min, recording for 5 min at each time point.

For the remainder of the experiments the cremaster muscle preparation was used. Firstly, the effect of L-NAME treatment was examined. After an initial 30 min stabilization period, the superfusion buffer was changed to one containing L-NAME (100 μM). Previous studies have demonstrated that this dose causes a consistent increase in leukocyte rolling and adhesion over a 60 min time course (Arndt *et al*., 1993). Recordings were performed at 15 min intervals over a 60 min period and leukocyte and haemodynamic parameters were measured at each time point.

To determine the role of nNOS in wild-type and eNOS$^{-/-}$ mice, an additional series of experiments were performed using the nNOS inhibitor, 7-nitroindazole, prepared as previously described (Alabadi *et al*., 1999) and administered at the same dose as L-NAME (100 μM in superfusion buffer). To demonstrate that this effect was NOS-dependent, another group of animals were pretreated with L-arginine (1 mg kg^{-1}, i.v.) 10 min prior to 7-nitroindazole superfusion. The dose of L-arginine used was the same employed by Davenpeck *et al*. (1994) to inhibit L-NAME-induced leukocyte-endothelial cell interactions in the rat mesenteric microcirculation.

H_2O_2 is an agonist known to induce NO release from endothelial cells. Therefore in a final series of experiments, we investigated the effect of H_2O_2 (100 μM) superfusion in both wild-type and eNOS$^{-/-}$ animals. H_2O_2 at this dose has been previously shown to cause a transient increase in leukocyte rolling in the rat mesenteric microcirculation (Johnston *et al*., 1996). Finally, another group of eNOS$^{-/-}$ animals were superfused with both H_2O_2 and 7-nitroindazole. Responses were determined at 15 min intervals over a 60 min period.

RT–PCR for nNOS gene expression

Brain and quadriceps muscle samples (200 mg) from eNOS$^{-/-}$ or from wild-type mice were taken and RNA extracted with TRIzol according to product instructions. Reverse transcription and polymerase chain reaction (RT–PCR) was performed using OneStep RT–PCR. The primer pairs were as follows: nNOS (Sense 5′–3′) GTCTTCCACCAGGAGATG and (Antisense 5′–3′) AAAGGCACAGAAGTGGGGGTA (Takimoto *et al*., 2000); and β-actin (Sense 5′–3′) CATGGATGATGATATCGCCG and (Antisense 5′–3′) ACAGCCTGGATAGCAACGTA. PCR products were at the size of 618 bp and 417 bp. The RT–PCR condition was optimized so that both nNOS and β-actin were expanding linearly, as follows: 50 ng total RNA, 0.4 μM of each nNOS primers, 0.2 μM of each β-actin primers and 35 cycles of PCR. PCR products were electrophoresed through a 2% agarose gel containing 0.5 μg/ml ethidium bromide. Bands were visualized and analysed using a Fluor-S MAX MultiImager and Quantity One software (Bio-Rad Laboratories, CA, USA).

Statistical analysis

All data are expressed as mean±s.e.mean. The data within groups were compared using an analysis of variance (one way-ANOVA) with a Bonferroni *post hoc* correction for multiple comparisons. A P value <0.05 was considered to be statistically significant.

Materials

L-NAME, 7-nitroindazole, fluorescein isothiocyanate (FITC)-labeled dextran (MW 150,000), L-arginine and rhodamine-6G were purchased from Sigma Chemical Co., St. Louis, MO, U.S.A. Xylazine hydrochloride was from MTC Pharmaceuticals, Cambridge, Ontario, Canada and ketamine hydrochloride was from Rogar/STB, London, Ontario, Canada. TRIzol was from GibcoBRL, NY, U.S.A. and OneStep RT–PCR kit was from Qiagen Inc., CA, U.S.A.

Results

Table 1 shows the different haemodynamic parameters in untreated wild-type and eNOS$^{-/-}$ mice at 0, 30 and 60 min after buffer superfusion. No significant differences in venular diameter, V_{rbc} or venular shear rate data were detected either between values obtained within the same group of animals at the different time periods of measurement or between the wild-type and the eNOS$^{-/-}$ mice. Figure 1 illustrates the changes in leukocyte rolling flux and the leukocyte adhesion in the cremaster muscle preparation at different time points

Table 1 Haemodynamic parameters 0, 30 and 60 min after buffer superfusion in wild-type and eNOS$^{-/-}$ mice

	0 min	*30 min*	*60 min*
Wild-type			
Venular diameter (μm)	29.8±1.6	30.6±1.6	30.3±1.6
V_{rbc} (mm s^{-1})	4.2±0.6	4.1±0.8	3.9±0.7
Shear rate (s^{-1})	773.9±140.0	708.9±157.9	668.0±138.5
eNOS$^{-/-}$			
Venular diameter (μm)	29.7±2.0	28.8±1.9	29.7±1.3
V_{rbc} (mm s^{-1})	3.4±0.7	3.3±0.7	2.9±0.3
Shear rate (s^{-1})	565.6±119.9	548.4±120.1	493.7±51.3

All values are mean±s.e.mean ($n=6$ wild-type animals and $n=10$ eNOS$^{-/-}$ mice).

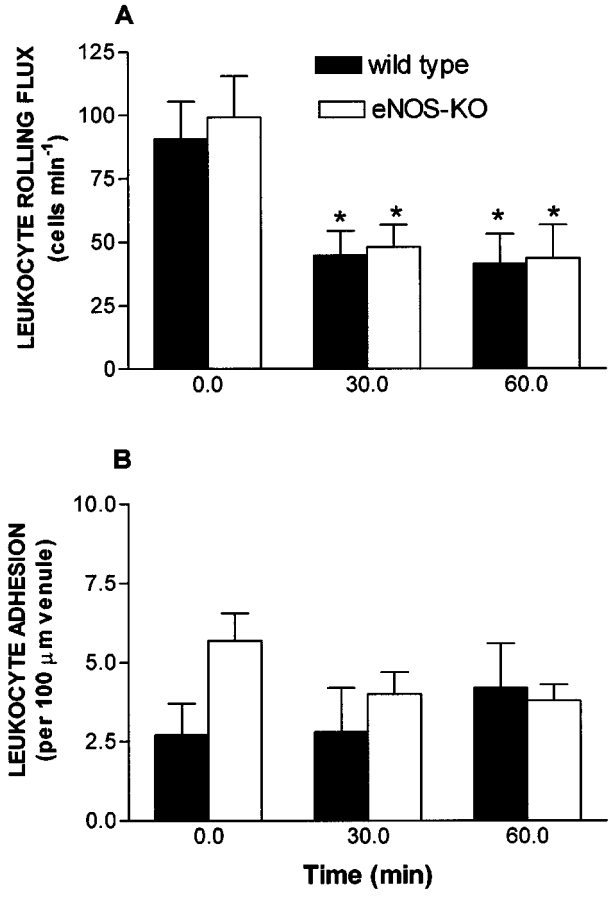

Figure 1 Baseline leukocyte rolling flux (A) and leukocyte adhesion (B) in the mouse cremasteric postcapillary venules in wild-type and eNOS$^{-/-}$ mice. The cremaster muscle was superfused with bicarbonate-buffered saline. Parameters were measured at 0, 30 and 60 min during buffer superfusion in wild-type ($n=6$) and eNOS$^{-/-}$ animals ($n=10$). Results are presented as mean$\pm$s.e.mean. *$P<0.05$ or **$P<0.01$ relative to the respective control value (0 min).

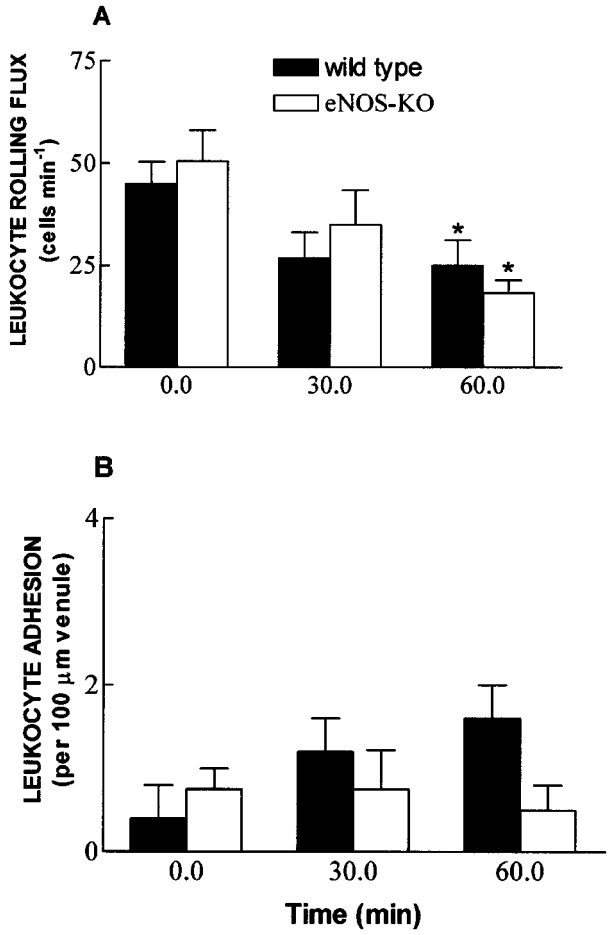

Figure 2 Baseline leukocyte rolling flux (A) and leukocyte adhesion (B) in the venules of the mouse small intestine submucosa in wild-type and eNOS$^{-/-}$ mice. After i.v. injection of FITC-dextran and rhodamine-6G, the small intestine submucosa was examined using epifluorescence microscopy. Parameters were measured at 0, 30 and 60 min in wild-type and eNOS$^{-/-}$ mice ($n=5$ per group). Results are presented as mean$\pm$s.e.mean. *$P<0.05$ or **$P<0.01$ relative to the respective control value (0 min).

under untreated conditions. No significant differences were observed between wild-type and eNOS$^{-/-}$ mice in both parameters at the different time points of measurement. As previously reported, a significant decrease in leukocyte rolling flux was detected in both animal groups with time. Although it appears that there may have been some subtle increase in spontaneous adhesion in eNOS$^{-/-}$ mice, the values are within acceptable levels for basal adhesion.

As others have reported baseline leukocyte differences in other organs, we examined baseline leukocyte rolling and adhesion under control conditions in another tissue, the submucosal microvasculature of the small intestine. The values obtained in this preparation followed a similar profile to that obtained in the cremasteric postcapillary venules, in that leukocyte rolling underwent a significant reduction over the course of the experiments. However, there were no significant differences in the number of rolling or adherent leukocytes between wild-type and eNOS$^{-/-}$ animals at 0, 30 and 60 min of buffer superfusion (Figure 2). On the basis of these preliminary results, all remaining experiments were performed in the cremaster muscle preparation and a 30 min stabilization period was allowed before determining basal measurements.

Figure 3 shows the time course of changes in leukocyte rolling flux and adhesion induced by L-NAME treatment of the cremaster in wild-type and eNOS$^{-/-}$ mice. Leukocyte rolling flux was unaltered by 60 min L-NAME treatment in both strains of mice. In contrast, L-NAME caused significant increases in leukocyte adhesion at 30 and 60 min in wild-type mice when compared with respective baseline values (10.9 ± 1.3 *vs* 2.6 ± 1.0 cells 100 μm^{-1} at 60 min). In eNOS$^{-/-}$ mice, leukocyte adhesion was also increased by L-NAME treatment (14.0 ± 3.7 *vs* 1.9 ± 0.4 cells 100 μm^{-1} at 60 min), such that no significant differences were observed between wild-type and mutant mice at any point after L-NAME superfusion.

To examine a role for nNOS in regulation of leukocyte rolling and adhesion, we next examined the effect of the nNOS selective inhibitor 7-nitroindazole in wild-type and eNOS$^{-/-}$ animals (Figure 4). 7-Nitroindazole had no effect on leukocyte rolling in either strain of mice. In wild-type mice leukocyte adhesion was also unaltered by this treatment. However in contrast, 7-nitroindazole significantly increased leukocyte adhesion in eNOS$^{-/-}$ mice within 15 min of

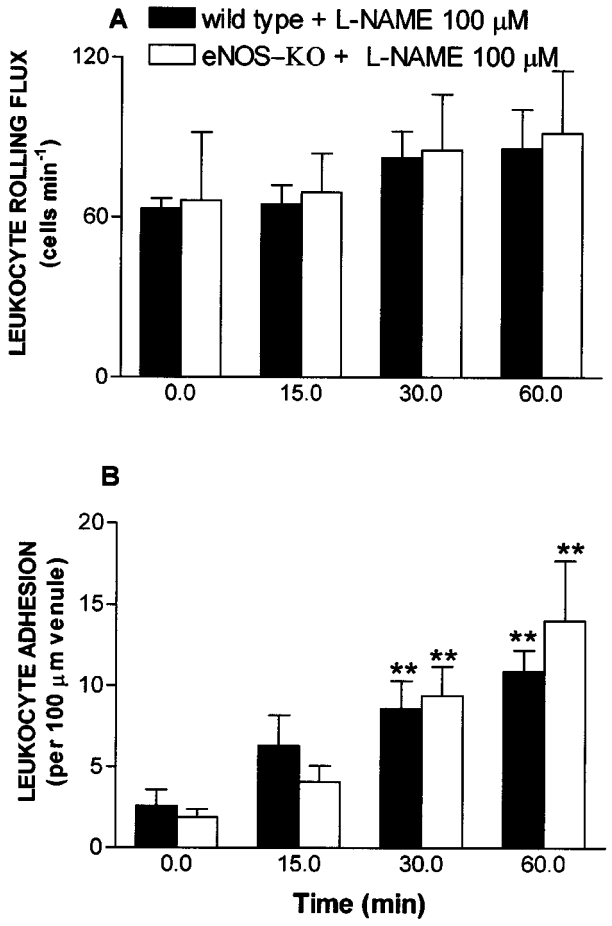

Figure 3 Effect of L-NAME on leukocyte rolling flux (A) and leukocyte adhesion (B) in the mouse cremasteric postcapillary venules in wild-type and $eNOS^{-/-}$ mice. The cremaster muscle was superfused with bicarbonate-buffered saline. After the 30 min stabilization period, the baseline parameters (0 min) were determined. Then superfusion buffer was supplemented with L-NAME (100 μM). Parameters were measured 0, 15, 30 and 60 min after superfusion with L-NAME in wild-type and $eNOS^{-/-}$ animals ($n=5$ in both groups). Results are presented as mean$\pm$s.e.mean. $^{*}P<0.05$ or $^{**}P<0.01$ relative to the respective control value (0 min).

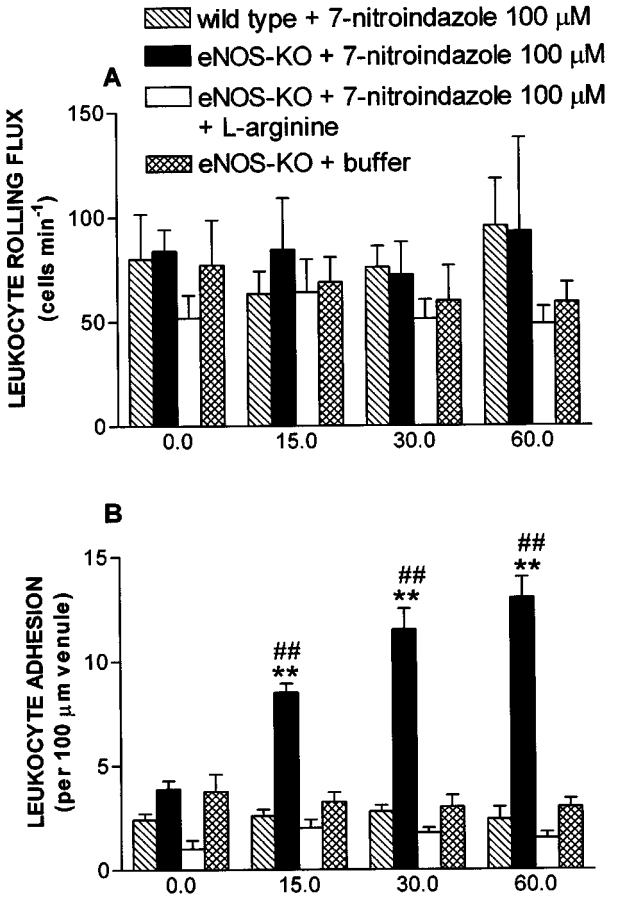

Figure 4 Effect of 7-nitroindazole on leukocyte rolling flux (A) and leukocyte adhesion (B) in the mouse cremasteric postcapillary venules in wild-type and $eNOS^{-/-}$ mice. Parameters were determined at 0, 15, 30 and 60 min after 7-nitroindazole (100 μM) superfusion in both wild-type and $eNOS^{-/-}$ mice ($n=4$ in both groups). In one group of $eNOS^{-/-}$ animals, L-arginine (1 mg kg^{-1}, i.v.) was administered 15 min prior 7-nitroindazole superfusion ($n=4$). Another group of $eNOS^{-/-}$ mice was superfused with buffer for the same period of time as 7-nitroindazole ($n=4$). Results are presented as mean$\pm$ s.e.mean. $^{*}P<0.05$ or $^{**}P<0.01$ relative to the respective control value (0 min). $\#P<0.01$ relative to values detected in wild-type animals.

beginning the treatment, with adhesion remaining significantly elevated out to 60 min (13.0 ± 1.0 *vs* 3.8 ± 0.4 cells 100 μm^{-1} venule at 60 min *vs* buffer alone). Pretreatment with L-arginine prevented the increase in leukocyte adhesion caused by 7-nitroindazole superfusion in $eNOS^{-/-}$ mice. In these animals, superfusion of the cremaster muscle with buffer for the same period as 7-nitroindazole caused no increases in leukocyte rolling flux and adhesion *versus* time 0 at the different time points determined.

To determine the effect of eNOS deficiency on leukocyte rolling, direct application of H_2O_2 (100 μM) to the cremaster muscle of wild-type and $eNOS^{-/-}$ mice was also performed (Figure 5). Figure 5A and B demonstrate typical responses to H_2O_2 administration in a wild-type and $eNOS^{-/-}$ mice respectively. Figure 5C shows the grouped data showing that H_2O_2 caused a significant and transient elevation in the leukocyte rolling flux in wild-type mice, returning to baseline levels by 30 min. In contrast, in $eNOS^{-/-}$ mice the H_2O_2 response persisted during the 60 min of experimental protocol. Furthermore, when the cremaster muscle was superfused with both H_2O_2 and 7-nitroindazole in $eNOS^{-/-}$ mice, responses at 15 min were also maintained throughout the entire experiment, indicating a prominent role for endothelial derived NO in the leukocyte rolling elicited by H_2O_2 superfusion. Leukocyte adhesion was unaffected by this treatment (data not shown). H_2O_2 caused no changes in venular diameter, V_{rbc} or venular shear rate throughout the entire experiment in either wild-type or $eNOS^{-/-}$ animals (Table 2).

Finally, as shown in figure 6, the semi-quantitative analysis of nNOS mRNA levels by RT–PCR showed that the expression of this enzyme was increased about 2 fold in the brain tissue of $eNOS^{-/-}$ mice compared with wild-type animals (the ratio nNOS/β Actin was 1.545 in wild-type mice and 3.154 in $eNOS^{-/-}$ mice) and 4 fold in the skeletal muscle of $eNOS^{-/-}$ mice compared with wild-type animals (the ratio nNOS/β Actin was 0.143 in wild-type mice and 0.621 $eNOS^{-/-}$ mice).

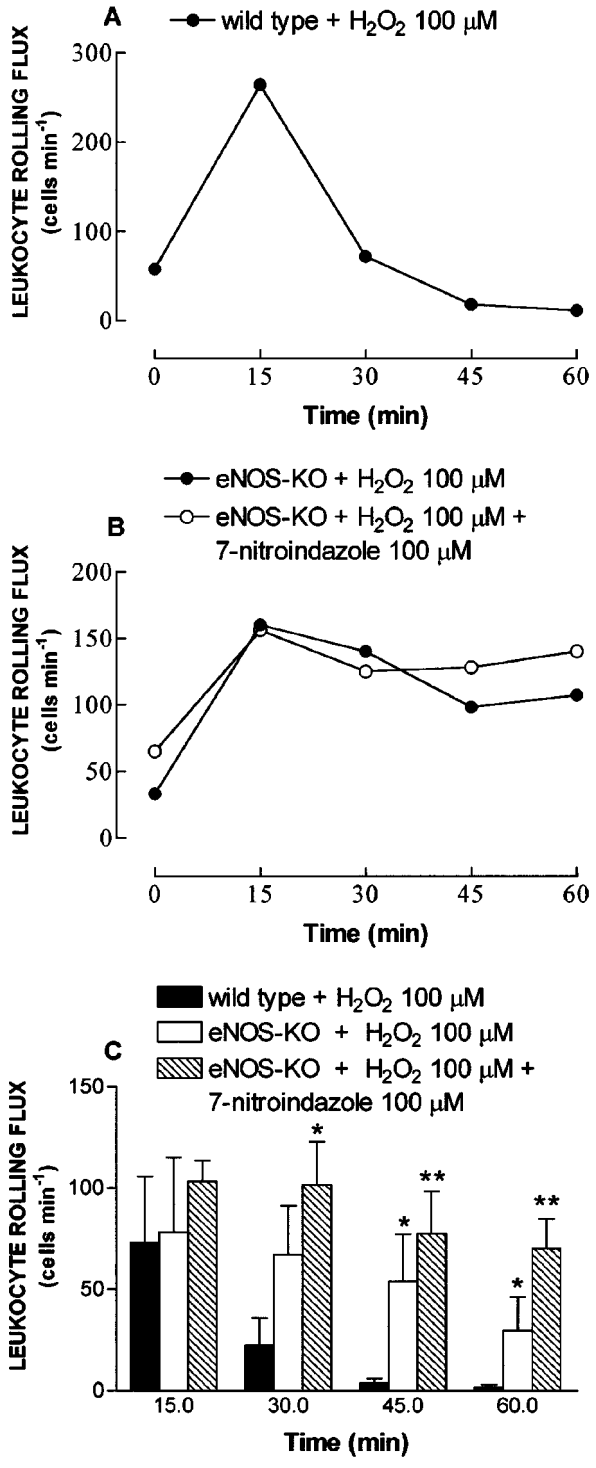

Figure 5 Effect of H_2O_2 on leukocyte rolling flux in the mouse cremasteric postcapillary venules in wild-type and eNOS$^{-/-}$ mice. Representative example of alterations in leukocyte rolling flux after H_2O_2 superfusion in a wild-type animal (A). Representative example of alterations in leukocyte rolling flux after H_2O_2 superfusion in eNOS$^{-/-}$ animal with or without 7-nitroindazole (B). After the 30 min stabilization period, the baseline values were determined (0 min). Parameters were measured 0, 15, 30, 45 and 60 min after superfusion with H_2O_2 (100 μM) in both wild-type and eNOS$^{-/-}$ mice and H_2O_2 and 7-nitroindazole (100 μM) in eNOS$^{-/-}$ mice ($n=6$ in all groups) (C). Results represents mean $\pm$ s.e.mean of the numbers obtained after subtracting respective basal values. *$P<0.05$ relative wild-type animal value at each time point.

Discussion

In the present study, to determine the specific contribution of endothelial and neuronal NOS isoforms in the modulation of leukocyte-endothelial cell interactions in the cremasteric microcirculation, we have used mice with targeted deletion of the former isoform. Surprisingly in light of previous studies, we observed no differences in baseline leukocyte rolling or adhesion between wild-type and eNOS$^{-/-}$ mice. Moreover we observed that inhibition of constitutive nitric oxide production with L-NAME, a non-selective NOS inhibitor, increased adhesion in eNOS$^{-/-}$ mice as well as wild-type mice. These findings suggested that an alternative NOS isoform was active in eNOS$^{-/-}$ mice. Therefore, to assess a role for nNOS, we examined the effect of the nNOS-selective inhibitor, 7-nitroindazole. In wild-type mice, this inhibitor had no effect on leukocyte adhesion. Taken together with the L-NAME data, this indicated that eNOS is the predominant isoform responsible for constitutive NO-mediated anti-adhesive activity in wild-type mice. However, 7-nitroindazole treatment dramatically increased adhesion in eNOS$^{-/-}$ mice, indicating a role for nNOS in modulation of leukocyte trafficking in the absence of eNOS. Furthermore, RT–PCR analysis in brain and skeletal muscle samples from both strains of mice, revealed increased RNAm of nNOS levels in brain and skeletal muscle of eNOS$^{-/-}$ animals. These experiments provide the first evidence that NO produced by nNOS is capable of substituting for the anti-leukocyte adhesion effects of eNOS-derived NO.

In this regard, our data do not agree with the recent findings of Lefer *et al.* (1999) who demonstrated significant differences in baseline leukocyte rolling and adhesion between the strains of mice in the mesenteric microcirculation. The lack of differences in both parameters in the mouse cremasteric microcirculation between wild-type and eNOS$^{-/-}$ animals prompted us to choose another vascular territory, the submucosal microvasculature of the small intestine. Indeed, recent studies have shown different behaviour for vasodilator responses in eNOS$^{-/-}$ mice depending on the vessel under investigation (Meng *et al.*, 1996; 1998, Huang *et al.*, 1995, Faraci *et al.*, 1998). Given these observations, it is conceivable that the control of leukocyte-endothelial cell interactions may also differ between different tissues. However, in our study, the intestinal submucosa also displayed no significant alterations of leukocyte trafficking in the absence of eNOS, consistent with the cremaster data.

Our work reveals that the lack of a different phenotype in eNOS$^{-/-}$ mice under basal conditions is due to nNOS. In this context, although the main NOS isoform in the endothelium is eNOS, recent studies have found that nNOS isoform can also be found in endothelial cells of different vascular territories and in the perivascular fibres surrounding these organs and that both are functionally important (Rosenblum & Murata, 1996; Loesch & Burnstock, 1995; 1998; Sosunov *et al.*, 1995). Hence, it might be possible that the mesenteric microcirculation in eNOS$^{-/-}$ mice has lower levels of nNOS than the cremasteric and small intestine submucosal vasculature and may explain the discrepant results in the two studies. Indeed, it has recently been found that other vasodilatory pathways in the mesentery were potassium-induced rather than NO-induced in eNOS$^{-/-}$ animals (Ding *et al.*, 2000).

Table 2 Haeodynamic parameters 15, 30, 45 and 60 min after H_2O_2 (100 μM) superfusion in wild-type and eNOS$^{-/-}$

	15 min	*30 min*	*45 min*	*60 min*
Wild-type				
Venular diameter (μm)	32.7±1.4	33.7±1.4	33.7±1.5	33.7±1.6
V_{rbc} (mm s^{-1})	3.4±0.5	2.9±0.3	2.7±0.4	3.1±0.4
Shear rate (s^{-1})	517.7±77.5	434.4±50.6	404.5±55.6	449.9±46.3
eNOS$^{-/-}$				
Venular diameter (μm)	37.7±2.5	39.5±3.3	38.8±3.2	39.7±3.2
V_{rbc} (mm s^{-1})	3.5±0.6	4.6±1.6	3.0±0.7	2.8±0.6
Shear rate (s^{-1})	479.8±80.1	648.7±260.4	399.1±84.4	346.5±59.1

All values are mean±s.e.mean ($n=6$ animals).

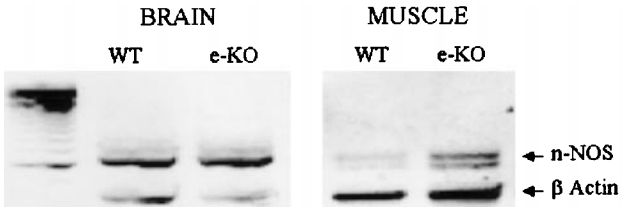

Figure 6 RT–PCR of nNOS and β Actin in brain and skeletal muscle tissue of wild-type animals and eNOS$^{-/-}$ mice. The ratio nNOS/β Actin was 1.545 in wild-type mice and 3.154 in eNOS$^{-/-}$ mice in brain tissue and 0.143 in wild-type mice and 0.621 eNOS$^{-/-}$ mice in the skeletal muscle tissue. Results presented are representative of $n=4$ experiments.

We were surprised to see that L-NAME induced a significant time-dependent increase in leukocyte adhesion regardless of the presence or absence of eNOS. This interesting finding led us to suspect that a compensating mechanism might be involved in these leukocyte responses. To test the hypothesis that neuronally derived NO plays a compensatory role in leukocyte responses in eNOS$^{-/-}$ mice, we evaluated the response to 7-nitroindazole. When 7-nitroindazole was superfused at the same dose as L-NAME, it had no effect on leukocyte rolling and adhesion in wild-type animals, but induced a marked increase in leukocyte adhesion in eNOS null mice. Interestingly, when animals were pretreated with L-arginine, leukocyte adhesion induced by 7-nitroindazole was abolished, indicating a NOS-dependent mechanism. Furthermore, nNOS expression was significantly enhanced in the brain and skeletal muscle of eNOS$^{-/-}$ mice.

After selective deletion of a gene, it is not uncommon for these mutant mice to display no or minimal differences in phenotype (Steinman, 1997). Indeed, recent studies suggest that, in the absence of eNOS, compensatory mechanisms may regulate vascular tone. In this context, mice that are deficient for the eNOS gene, NO-dependent-acetylcholine-induced dilatation of cerebral arterioles has been reported to be unaltered from that observed in wild-type mice (Meng *et al*., 1998; 1996), implying a role for an alternative NOS isoform. Similarly, penile vasodilatation due to NO from inhibitory nerves was initially thought to be the main factor in penile erection. However, penile erection was not affected in nNOS$^{-/-}$ mice, yet the erection in nNOS$^{-/-}$ mice was sensitive to NOS inhibition (Burnett *et al*., 1996). Our results further demonstrate a crucial role for nNOS in the modulation of leukocyte responses when eNOS is absent and, the possible contribution of inducible NOS (iNOS) seems quite unlikely, since it requires hours to be up-regulated (Morris & Billiar, 1994). In addition, a nNOS selective inhibitor entirely reproduced the effects of a non specific NOS inhibitor. This is of interest since often these compensatory pathways reveal novel functions for proteins in the normal (non-mutated) systems.

Despite these findings, nNOS was unable to fully compensate for eNOS. When H_2O_2 was superfused in the cremasteric preparation, it elicited a rapid and transient increase in leukocyte rolling flux in wild-type animals, however, this increase was maintained during the whole experimental period in eNOS$^{-/-}$ mice either with or without 7-nitroindazole. These results suggest that endothelial derived NO is necessary to scavenge oxidants and protect the cells from H_2O_2-induced damage. In support of this view, Johnston *et al*. (1996) demonstrated a similar effect in the rat mesenteric microcirculation upon H_2O_2 superfusion and NOS inhibition with L-NAME. H_2O_2 stimulates endothelial cells to release NO (Zembowicz *et al*., 1993), and thus it explains the transient increase in leukocyte rolling observed in the rat mesenteric microcirculation or in the cremasteric microcirculation of wild-type animals in our study. Furthermore, it is estimated that neutrophils that have emigrated out of the blood vessels can generate local concentrations of 200–500 μM H_2O_2 within 60 min of stimulation (Grisham *et al*., 1990). These findings indicate that the concentration of H_2O_2 used both in the present and by Johnston *et al*. (1996) is physiologically relevant in the context of an inflammatory response. Nevertheless, whether NO released by H_2O_2 was from neuronal or endothelial origin remained undetermined in that study due to the lack of selective eNOS inhibitors available at that time. In the present study and using eNOS null mice, we have demonstrated that NO released upon H_2O_2 stimulation is predominantly from endothelial origin.

In conclusion, the present study is the first to demonstrate that under baseline conditions, leukocyte-endothelial cell interactions in postcapillary venules are predominantly modulated by eNOS in normal (wild-type) mice. However, in eNOS$^{-/-}$ mice this function is mediated exclusively by nNOS. Interestingly, unlike eNOS there was insufficient NO produced by nNOS to overcome leukocyte recruitment elicited by oxidative stress, suggesting that nNOS cannot completely compensate for eNOS.

M.J. Sanz was supported by a grant from Conselleria de Educación y Ciencia (Generalitat Valenciana). M.J. Hickey was supported by an MRC/Canadian Association for Gastroenterology/Astra fellowship. P. Kubes is an Alberta Heritage Foundation for Medical Research Scientist and a MRC scientist. This work was also supported by grant PM 98 205 from CYCIT, Spanish Ministerio de Educación y Ciencia.

References

ALABADI, J.A., THIBAULT, J.L., PINARD, E., SEYLAZ, J. & LASBENNES, F. (1999). 7-Nitroindazole, a selective inhibitor of nNOS, increases hippocampal extracellular glutamate concentration in status epilepticus induced by kainic acid in rats. *Brain Res.,* **839,** 305–312.

ARNDT, H., RUSSELL, J.B., KUROSE, I., KUBES, P. & GRANGER, D.N. (1993). Mediators of leukocyte adhesion in rat mesenteric venules elicited by inhibition of nitric oxide synthesis. *Gastroenterology,* **105,** 675–680.

BURNETT, A.L., NELSON, R.J., CALVIN, D.C., LIU, J.X., DEMAS, G.E., KLEIN, S.L., KRIEGSFELD, L.J., DAWSON, V.L., DAWSON, T.M. & SNYDER, S.H. (1996). Nitric oxide-dependent penile erection in mice lacking neuronal nitric oxide synthase. *Mol. Med.,* **2,** 288–296.

DAVENPECK, K.L., GAUTHIER, T.W. & LEFER, A.M. (1994). Inhibition of endothelial-derived nitric oxide promotes P-selectin expression and actions in the rat microcirculation. *Gastroenterology,* **107,** 1050–1058.

DING, H., KUBES, P. & TRIGGLE, C. (2000). Potassium- and acetylcholine-induced vasorelaxation in mice lacking endothelial nitric oxide synthase. *Br. J. Pharmacol.,* **129,** 1194–1200.

FARACI, F.M., SIGMUND, C.D., SHESELY, E.G., MAEDA, N. & HEISTAD, D.D. (1998). Responses of carotid artery in mice deficient in expression of the gene for endothelial NO synthase. *Am. J. Physiol.,* **274,** H564–H570.

GABOURY, J.P., WOODMAN, R.C., GRANGER, D.N., REINHARDT, P. & KUBES, P. (1993). Nitric oxide prevents leukocyte adherence: role of superoxide. *Am. J. Physiol.,* **265,** H862–H867.

GRISHAM, M.B., GAGINELLA, T.S., VON RITTER, C., TAMAI, H., BE, R.M. & GRANGER, D.N. (1990). Effects of neutrophil-derived oxidants on intestinal permeability, electrolyte transport, and endothelial cell viability. *Inflammation,* **14,** 531–542.

HICKEY, M.J., GRANGER, D.N. & KUBES, P. (1999). Molecular mechanisms underlying IL-4-induced leukocyte recruitment in vivo: a critical role for the α_4 integrin. *J. Immunol.,* **163,** 3441–3448.

HOUSE, S.D. & LIPOWSKY, H.H. (1987). Leukocyte-endothelium adhesion: microhemodynamics in mesentery of the cat. *Microvasc. Res.,* **34,** 363–379.

HUANG, P.L., HUANG, Z., MAHIMO, H., BLOCH, K.D., MOSCOWITZ, M.A., BEVAN, J.A. & FISHMAN, M.C. (1995). Hypertension in mice lacking the gene for endothelial cell nitric oxide synthase. *Nature,* **377,** 239–242.

HUANG, Z., HUANG, P.L., PANAHIAN, N., DALKARA, T., FISHMAN, M.C. & MOSCOWITZ, M.A. (1994). Effects of cerebral ischemia in mice deficient in neuronal nitric oxide synthase. *Science,* **265,** 1883–1885.

JOHNSTON, B., KANWAR, S. & KUBES, P. (1996). Hydrogen peroxide induces leukocyte rolling: modulation by endogenous antioxidant mechanisms including NO. *Am. J. Physiol.,* **271,** H614–H621.

JONES, S.P., GIROD, W.G., PALAZZO, A.J., GRANGER, D.N., GRISHAM, M.B., JOURD'HEUIL, D., HUANG, P.L. & LEFER, D.J. (1999). Myocardial ischemia-reperfusion injury is exacerbated in absence of endothelial cell nitric oxide synthase. *Am. J. Physiol.,* **276,** H1567–H1573.

KUBES, P., KANWAR, S., NIU, X.F. & GABOURY, J.P. (1993). Nitric oxide synthesis inhibitors induce leukocyte adhesion via superoxide and mast cells. *FASEB J.,* **7,** 1293–1299.

KUBES, P., SUZUKI, M. & GRANGER, D.N. (1991). Nitric oxide: an endogenous modulator of leukocyte adhesion. *Proc. Natl. Acad. Sci. U.S.A.,* **88,** 4651–4655.

LEFER, D.J., JONES, S.P., GIROD, W.G., BAINES, A., GRISHAM, M.B., COCKRELL, A.S., HUANG, P.L. & SCALIA, R. (1999). Leukocyte-endothelial cell interactions in nitric oxide synthase-deficient mice. *Am. J. Physiol.,* **276,** H1943–H1950.

LOESCH, A. & BURNSTOCK, G. (1995). Ultrastructural localization of nitric oxide synthase and endothelin in coronary and pulmonary arteries of newborn rats. *Cell Tissue Res.,* **279,** 475–483.

LOESCH, A. & BURNSTOCK, G. (1998). Perivascular nerve fibres and endothelial cells of the rat basilar artery: immuno-gold labelling of antigenic sites for type I and type III nitric oxide synthase. *J. Neurocytol.,* **27,** 197–204.

MASSBERG, S., EISENMENGER, S., ENDERS, G., KROMBACH, F. & MESSMER, K. (1998). Quantitative analysis of small intestinal microcirculation in the mouse. *Res. Exp. Med.,* **198,** 23–35.

MENG, W., AYATA, C., WAEBER, C., HUANG, P.L. & MOSKOWITZ, M.A. (1998). Neuronal NOS-cGMP-dependent Ach-induced relaxation in pial arterioles of endothelial NOS knockout mice. *Am. J. Physiol.,* **274,** H411–H415.

MENG, W., MA, J., AYATA, C., HARA, H., HUANG, P.L., FISHMAN, M.C. & MOSKOWITZ, M.A. (1996). Ach dilates pial arterioles in endothelial and neuronal NOS knockout mice by NO-dependent mechanism. *Am. J. Physiol.,* **271,** H1145–H1150.

MONCADA, S., PALMER, R.M.J. & HIGGS, E.A. (1991). Nitric oxide: physiology, pathophysiology, and pharmacology. *Pharmacol. Rev.,* **43,** 109–142.

MORRIS, S.M. & BILLIAR, T.R. (1994). New insights into the regulation of inducible nitric oxide synthesis. *Am. J. Physiol.,* **266,** E829–E839.

NIU, X.F., IBBOTSON, G. & KUBES, P. (1996). A balance between nitric oxide and oxidants regulates mast cell-dependent neutrophil-endothelial cell interactions. *Circ. Res.,* **79,** 992–999.

RADOMSKI, M.W., PALMER, R.M.J. & MONCADA, S. (1987). The anti-aggregating properties of vascular endothelium: interaction between prostacyclin and nitric oxide. *Br. J. Pharmacol.,* **92,** 639–646.

ROSENBLUM, W.I. & MURATA, S. (1996). Antisense evidence for two functionally active forms of nitric oxide synthase in brain microvascular endothelium. *Biochem. Biophys. Res. Commun.,* **224,** 535–543.

SOSUNOV, A.A., HASSALL, C.J., LOESCH, A., TURMAINE, M. & BURNSTOCK, G. (1995). Ultrastructural localization of nitric oxide synthase-immunoreactive nerves associated with coronary blood vessels of rat and guinea-pig. *Cell Tissue Res.,* **280,** 575–582.

STEINMAN, L. (1997). Some misconceptions about understanding auto-immunity through experiments with knockouts. *J. Exp. Med.,* **185,** 2039–2041.

TAKIMOTO, Y., AOYAMA, T., KEYAMURA, R., SHINODA, E., HATTORI, R., YUI, Y. & SASAYAMA, S. (2000). Differential expression of three types of nitric oxide synthase in both infarcted and non-infarcted left ventricle after myocardial infarction in the rat. *Int. J. Cardiol.,* **76,** 135–145.

ZEMBOWICZ, A., HATCHETT, R.J., JAKUBOWSKI, A.M. & GRYGLEWSKI, R.J. (1993). Involvement of nitric oxide in the endothelium-dependent relaxation induced by hydrogen peroxide in the rabbit aorta. *Br. J. Pharmacol.,* **110,** 151–158.

(Received May 11, 2001
Accepted May 20, 2001)